

Quantum Chemical Studies on Structures of 1-Isopropyl -4-Methylbenzene

G.Vijayakumar* and N.Saravanan

Department of Chemistry A.A. Government Arts College, Musiri- 621 211, Tamil Nadu, India.

ARTICLE INFO

Article history:

Received: 2 April 2016;

Received in revised form:

1 May 2016;

Accepted: 6 May 2016;

Keywords

FT-IR,
FT-Raman,
IMB,
HF,
DFT,
NLO,
HOMO-LUMO.

ABSTRACT

The vibrational spectroscopy of 1-isopropyl-4-methyl benzene [IMB] by means of quantum chemical calculation has been studied. The FT-Raman and FT-IR spectra of IMB have been recorded in the region $3500-50\text{cm}^{-1}$ and $4000-400\text{cm}^{-1}$ respectively. The fundamental vibrational frequencies and intensity of vibrational bands have been evaluated using HF and density functional theory (DFT) with standard B3LYP/6-311++G(d,p) and HF/6-311++G(d,p) basis set combinations for optimized geometries. The observed FT-IR and FT-Raman vibrational frequencies have been analysed and compared with theoretically predicted vibrational frequencies. The assignments of bands to various normal modes of molecule have also been carried out. The electric dipole moment (μ) and the first hyperpolarizability (β) values of the investigated molecule have been computed using DFT calculations. The calculated HOMO and LUMO energies show that charge transfer occur with in the molecule.

© 2016 Elixir All rights reserved.

1. Introduction

Benzene is mainly used as an intermediate to make other chemicals. Its most widely produced derivatives include styrene, which is used to make polymers and plastics, phenol for resins and adhesives, and cyclohexane, which is used in the manufacture of Nylon [1]. Nitrobenzene, the simplest nitro aromatic compound, is the parent compound of a range of important compounds, including explosives; 2,4,6-trinitrotoluene. It is also related to nitro phenols, including the biologically important nitro tyrosine, whose presence in proteins is often the result of damage by peroxynitrite [2-4]. A full theoretical understanding of the molecular properties of nitrobenzene can therefore inform on the properties of these other larger compounds. The vibrational spectroscopy of nitrobenzene has been the subject of numerous studies [5,6].

Benzene and its derivatives do not undergo most of the usual addition reactions of alkenes. Instead, they undergo reactions in which another group substitutes ring hydrogen. Such substitution reaction can be used to prepare a variety of substituted benzene from benzene itself. One of the most characteristic reactions of benzene and many of its derivatives is substitution of ring hydrogen by an electrophile and reactions of this type are often called as electrophilic aromatic substitution reactions. Both activating/deactivating and directing effects of substituents come into play in planning an organic synthesis that involves electrophilic substitution reactions.

Hence the understanding of molecular properties as well as the nature of reaction mechanism they undergo has great importance. The substituted benzene derivatives with high optical non-linearity are very promising materials for future optoelectronics and non-linear optical applications. Non-linear optical effects of compound depend on the polarizability of organic material is generally contribution from the lattice components because of the weak intermolecular bonding and

hence possesses the high degree of delocalization. By combining all these facts into account, the present study has been aimed, to investigate the vibrational spectra of 1-Isopropyl-4-methylbenzene (IMB). Investigations have also been carried out to analyse the HOMO-LUMO energy gap and NLO property (first-hyperpolarizability). All these investigations have been done on the basis of the optimized geometry by using Hartree fock and density functional theory (DFT) at HF/B3LYP/6-311++G(d,p) level.

2. Experimental details

The pure sample of 1-Isopropyl-4-methylbenzene (IMB) was obtained from Lancaster Company, UK that is of spectroscopic grade and hence used for recording the spectra as such without any further purification. The FT-IR spectra of IMB was measured in the BRUKER IFS 66V spectrometer in the range $4000-400\text{cm}^{-1}$. The FT-Raman spectra of IMB was also recorded in FT-Raman BRUKER RFS 100/S instrument equipped with Nd:YAG laser source operating at 1064 nm line widths with 150 mW powers. The spectrum is recorded in the range $3500-50\text{cm}^{-1}$. The spectral resolution is $\pm 4\text{cm}^{-1}$.

3. Methods of Computation

The initial geometries of IMB were optimized using the HF/B3LYP/6-311++G(d,p) level of Gaussian 09W program package [7]. The vibrational frequency analysis was computed using HF/B3LYP/6-311++G(d,p) method to determine the nature of a stationary point found by geometry optimization. HOMO-LUMO analysis has been carried out to explain the charge transfer within the compounds. The chemical hardness (η) and chemical potential (μ) have been calculated using the Highest occupied molecular orbital (HOMO) and Lowest unoccupied molecular orbital (LUMO) energies. NBO analysis has also been performed using B3LYP/6-311++G(d,p) level in order to elucidate the intermolecular hydrogen bonding, intermolecular charge transfer (ICT), rehybridization, delocalization of electron density.

Tele:

E-mail address: n79saravanan@gmail.com

© 2016 Elixir All rights reserved

Table 1. Optimized geometrical parameters of 1-isopropyl 4-methyl benzene obtained by HF/6-31++G(d,p) and B3LYP/6-31++G(d,p) methods and basis set.

Bond length	Value (Å)		Bond angle	Value (°)		Dihedral angle	Value (°)	
	6-31+G(d,p)			6-31+G(d,p)			6-31+G(d,p)	
	HF	B3LYP		HF	B3LYP		HF	B3LYP
C1-C2	1.3896	1.4039	C2-C1-C6	117.4823	117.608	C6-C1-C2-C3	-0.0008	0.002
C1-C6	1.3969	1.4088	C2-C1-C7	120.7726	120.8405	C6-C1-C2-H8	180.0002	179.9991
C1-C7	1.522	1.5267	C6-C1-C7	121.7451	121.5515	C7-C1-C2-C3	179.9991	179.9999
C2-C3	1.3925	1.4024	C1-C2-C3	121.372	121.2876	C7-C1-C2-H8	0.0001	-0.0031
C2-H8	1.0749	1.0875	C1-C2-H8	119.5217	119.3433	C2-C1-C6-C5	0.0002	-0.0005
C3-C4	1.3887	1.4037	C3-C2-H8	119.1063	119.3691	C2-C1-C6-H12	179.9996	179.9998
C3-H9	1.0747	1.0872	C2-C3-C4	121.0622	121.0597	C7-C1-C6-C5	-179.9998	-179.9984
C4-C5	1.3961	1.4084	C2-C3-H9	119.2625	119.4726	C7-C1-C6-H12	-0.0004	0.0019
C4-C10	1.5104	1.5141	C4-C3-H9	119.6753	119.4677	C2-C1-C7-H13	-0.0018	0.0007
C5-C6	1.3855	1.398	C3-C4-C5	117.6756	117.7229	C2-C1-C7-C17	117.3347	117.4345
C5-H11	1.0754	1.0877	C3-C4-H10	121.6029	121.4598	C2-C1-C7-C18	-117.3378	-117.429
C6-H12	1.0742	1.0868	C5-C4-H10	120.7215	120.8172	C6-C1-C7-H13	-180.0018	179.9985
C7-H13	1.0869	1.1002	C4-C5-C6	121.2242	121.1818	C6-C1-C7-C17	-62.6653	-62.5677
C7-H17	1.5386	1.5471	C4-C5-H11	119.457	119.3945	C6-C1-C7-C18	62.6621	62.5688
C7-H18	1.5386	1.5472	C6-C5-H11	119.3188	119.4237	C1-C2-C3-C4	0.0003	-0.0024
C10-H14	1.0831	1.0951	C1-C6-C5	121.1837	121.1399	C1-C2-C3-H9	180.0006	179.9986
C10-H15	1.0851	1.0978	C1-C6-H12	119.9532	119.8341	H8-C2-C3-C4	-180.0007	-179.9994
10-H16	1.0851	1.0978	C5-C6-H12	118.8631	119.026	H8-C2-C3-H9	-0.0004	0.0016
C17-H19	1.084	1.096	C1-C7-H13	106.9208	106.9766	C2-C3-C4-C5	0.0009	0.0012
C17-H20	1.0847	1.0972	C1-C7-H17	111.9997	111.9889	C2-C3-C4-C10	179.9973	179.9985
C17-H21	1.0854	1.0973	C1-C7-H18	111.9993	111.9874	H9-C3-C4-C5	-179.99944	-179.9998
C18-H22	1.084	1.096	H13-C7-H17	107.3566	107.4135	H9-C3-C4-C10	-0.003	-0.0025
C18-H23	1.0854	1.0973	H13-C7-H18	107.3564	107.4109	C3-C4-C5-C6	-0.0016	0.0003
C18-H24	1.0847	1.0972	C17-C7-C18	110.9027	110.7725	C3-C4-C5-H11	180.0003	179.9994
			C4-C10-H14	111.1605	111.2556	C10-C4-C5-C6	180.002	-179.997
			C4-C10-H15	111.2242	111.4124	C10-C4-C5-H11	0.0038	0.002
			C4-C10-H16	111.2237	111.4124	C3-C4-C10-H14	0.0213	0.0327
			H14-C10-H15	107.757	107.6886	C3-C4-C10-H15	120.0977	120.2139
			H14-C10-H16	107.7566	107.687	C3-C4-C10-H16	-120.0543	-120.1463
			H15-C10-H16	107.5429	107.1785	C5-C4-C10-H14	180.0176	-179.97
			C7-C17-H19	111.0398	111.1225	C5-C4-C10-H15	-59.9059	-59.7889
			C7-C17-H20	111.2985	111.075	C5-C4-C10-H16	59.942	59.8509
			C7-C17-H21	110.4536	110.51	C4-C5-C6-C1	0.001	-0.0006
			H19-C17-H20	107.9207	107.879	C4-C5-C6-H12	-179.9984	179.9991
			H19-C17-H21	108.2194	108.3163	H11-C5-C6-C1	-180.0008	-179.9997
			H20-C17-H21	107.7792	107.8125	H11-C5-C6-H12	-0.0002	0.0
			C7-C18-H22	111.0395	111.1219	C1-C7-C17-H19	-55.9128	-56.1381
			C7-C18-H23	110.4535	110.5096	C1-C7-C17-H20	64.3395	63.967
			C7-C18-H24	111.2983	111.0734	C1-C7-C17-H21	-175.9786	-176.4174
			H22-C18-H23	108.2196	108.3178	H13-C7-C17-H19	61.1622	61.0337
			H22-C18-H24	107.9209	107.8792	H13-C7-C17-H20	-178.5855	-178.8612
			H23-C18-H24	107.7793	107.8137	H13-C7-C17-H21	-58.9035	-59.2456
						C18-C7-C17-H19	178.1585	178.0578
						C18-C7-C17-H20	-61.5892	-61.8371
						C18-C7-C17-H21	58.0927	57.7785
						C1-C7-C18-H22	55.9125	56.1534
						C1C7-C18-H23	175.9783	176.4338
						C1-C1-C18-H24	-64.3398	-63.9505
						H13-C7-C18-H22	-61.1623	-61.0159
						H13-C7-C18-H23	58.9035	59.2644
						H13-C7-C18-H24	178.5855	178.8802
						C17-C7-C18-H22	-178.1586	-178.0417
						C17-C7-C18-H23	-58.0928	-57.7613
						C17-C7-C18-H24	61.5892	61.8544

For numbering of atoms refer Fig. 1

Table 2. Vibrational assignments of fundamental modes of 1-isopropyl -4- methyl benzene along with calculated IR intensity (km mol^{-1}), Raman activity ($\text{Å}^4 \text{amu}^{-1}$) and normal mode descriptions (characterized by TED) based on quantum mechanical force field calculations using HF and B3LYP methods.

S. No.	Species	Observed fundamentals (cm^{-1})		Calculated frequencies (cm^{-1})								Assignments with TED (%) among types of internal coordinates
		FTIR	FT-Raman	HF/6-311++G(d,p)				B3LYP/6-311+ +G(d,p)				
				Unscaled ν_i	Scaled	IR intensity	Raman activity	Unscaled ν_i	Scaled	IR intensity	Raman activity	
1.	A	3490	-	3363	3498	3.9465	213.3752	3197	3493	2.2265	255.8313	$\gamma\text{CH}(99)$
2.	A	3120	-	3358	3127	54.5583	31.3756	3192	3122	57.2060	22.6741	$\gamma\text{CH}(98)$
3.	A	-	3080	3337	3087	14.9095	61.4771	3173	3081	10.5113	86.1609	$\gamma\text{CH}(97)$
4.	A	3050	-	3335	3058	19.7879	54.8271	3173	3055	23.6617	41.8642	$\gamma\text{CH}(98)$
5.	A	3030	-	3261	3039	27.9113	64.0723	3117	3033	23.1260	64.1289	$\gamma\text{CH}(98)$
6.	A	-	3020	3259	3031	51.3253	61.8687	3115	3026	38.0974	82.8452	$\gamma\text{CH}(98)$
7.	A	-	2970	3255	2972	28.7072	35.0827	3112	2971	26.7513	35.3992	$\text{CH}_3\text{ips}(80)+\gamma\text{CH}(20)$
8.	A	2960	-	3249	2968	111.5487	182.6562	3106	2962	100.4246	188.4326	$\text{CH}_3\text{ ips}(79)+\gamma\text{CH}(21)$
9.	A	-	2940	3240	2947	1.9255	10.6103	3098	2943	0.0248	10.3072	$\text{CH}_3\text{ips}(79)+\gamma\text{CH}(21)$
10.	A	2930	-	3237	2937	25.8377	87.8883	3087	2933	21.0853	95.7567	$\gamma\text{CH}(85)+\text{CH}_3\text{ss}(15)$
11.	A	-	2890	3185	2899	29.4688	414.6668	3036	2895	35.8240	388.1811	$\text{CH}_3\text{ss}(97)$
12.	A	2880	-	3183	2887	64.4610	111.7078	3033	2882	54.4523	197.0593	$\text{CH}_3\text{ss}(89)+\gamma\text{CH}(11)$
13.	A	-	2750	3179	2756	40.1210	2.4680	3031	2751	36.6581	4.1551	$\text{CH}_3\text{ss}(89)+\gamma\text{CH}(11)$
14.	A	2740	-	3173	2746	21.4724	58.3876	3018	2744	20.9171	76.4338	$\text{CH}_3\text{ops}(89)$
15.	A	2600	-	1812	2613	0.2955	37.2078	1664	2611	0.3111	52.1084	$\text{CH}_3\text{ops}(89)$
16.	A	1900	-	1761	1911	0.4636	8.4807	1621	1907	0.6802	6.5837	$\text{CH}_3\text{ops}(89)$
17.	A	1790	-	1693	1799	31.5672	0.7888	1565	1794	31.2731	1.2414	$\gamma\text{C}=\text{C}(90)$
18.	A	1700	-	1657	1707	7.7936	3.1486	1543	1703	7.1706	2.7490	$\gamma\text{C}=\text{C}(89)+\text{CH}_3\text{ipb}(12)$
19.	A	1640	-	1654	1648	8.7755	23.3190	1539	1645	9.6436	20.1127	$\gamma\text{C}=\text{C}(87)+\text{CH}_3\text{ipb}(13)$
20.	A	1620	-	1648	1629	17.1363	7.8840	1532	1626	16.5763	9.9203	$\gamma\text{C}-\text{C}(87)$
21.	A	-	1610	1643	1615	6.8684	14.7346	1528	1613	8.6731	12.4100	$\gamma\text{C}-\text{C}(89)$
22.	A	-	1580	1643	1586	5.9124	0.9348	1527	1582	5.6131	1.5808	$\text{CH}_3\text{ipb}(89)$
23.	A	1570	-	1639	1577	0.0634	20.4010	1526	1574	0.0004	16.4125	$\text{CH}_3\text{ipb}(90)+\gamma\text{C}-\text{C}(10)$
24.	A	1510	-	1583	1518	6.6379	1.5544	1464	1513	2.9658	1.1854	$\gamma\text{C}-\text{C}(89)$
25.	A	-	1470	1579	1475	5.0850	11.5757	1457	1471	4.6308	25.2825	$\gamma\text{C}-\text{C}(78)$
26.	A	1460	-	1578	1464	1.2620	1.1885	1455	1462	4.8377	0.3384	$\gamma\text{C}-\text{C}(76)$
27.	A	1410	-	1559	1419	9.6269	0.8377	1437	1415	9.2086	1.3808	$\text{CH}_3\text{ipb}(79)$
28.	A	1380	-	1519	1387	1.9118	0.9852	1404	1385	2.2061	1.4621	$\text{bCH}(78)+\text{CH}_3\text{ipb}(12)$
29.	A	-	1370	1483	1374	1.5596	9.2471	1368	1373	2.7535	1.9338	$\text{bCH}(78)$
30.	A	1360	-	1463	1366	5.9132	2.2046	1366	1364	2.7250	8.3212	$\text{bCH}(78)$
31.	A	1330	-	1372	1341	1.0681	2.2496	1333	1335	3.2412	1.0016	$\text{bCH}(79)$
32.	A	1310	-	1348	1314	0.7469	8.1881	1260	1311	0.0480	4.7245	$\text{CH}_3\text{sb}(79)$
33.	A	-	1300	1333	1309	0.0117	2.3807	1245	1306	3.5289	30.6312	$\text{CH}_3\text{sb}(80)$
34.	A	-	1280	1332	1288	4.4903	19.4434	1238	1285	1.7848	15.3921	$\text{CH}_3\text{sb}(81)$
35.	A	1270	-	1284	1276	0.6142	1.6713	1200	1271	0.9446	0.5002	$\text{bCH}(90)$
36.	A	1240	-	1235	1248	8.0827	1.4298	1158	1246	7.4782	2.8855	$\text{bCH}(90)$
37.	A	-	1210	1233	1217	1.2710	6.8054	1135	1214	1.4888	6.2581	$\text{bCH}(91)$
38.	A	1220	-	1210	1229	4.4356	0.1634	1099	1225	4.9888	0.0053	$\text{RSymd}(82)+\text{CH}_3\text{ipr}(18)$
39.	A	1200	-	1185	1205	15.8010	12.2998	1097	1201	17.8313	13.2627	$\text{CH}_3\text{ipr}(85)+\text{RSymd}(15)$
40.	A	-	1190	1153	1194	0.0187	0.0017	1055	1193	3.7198	0.0462	$\text{CH}_3\text{ipr}(85)$
41.	A	1180	-	1139	1187	2.2685	0.0726	1029	1182	0.2188	0.7635	$\text{RSymd}(85)$
42.	A	1150	-	1128	1155	1.6745	0.0595	1002	1153	0.0001	0.0808	$\text{CH}_3\text{ipr}(87)$
43.		1130	-	1106	1137	0.0508	1.0904	989	1135	0.4894	0.0089	$\text{Rtrigd}(87)$
44.		-	1110	1054	1121	0.0435	7.7454	981	1118	0.1148	6.3274	$\text{CH}_3\text{opb}(85)$
45.		1100	-	1032	1109	1.1895	3.2701	954	1107	0.7881	2.2396	$\text{CH}_3\text{opb}(84)$
46.		-	1060	982	1066	0.0754	0.7347	904	1064	0.5685	6.9761	$\text{CH}_3\text{opb}(84)$
47.		1050	-	966	1055	0.270	8.6683	869	1052	0.0475	0.4883	$\omega\text{CH}(75)$
48.		1010	-	959	1017	58.0740	0.5427	852	1013	43.2835	0.1875	$\omega\text{CH}(79)+\text{bCC}(21)$
49.		-	960	883	969	0.0849	45.3606	828	964	0.0343	37.1796	$\omega\text{CH}(79)+\text{bCC}(21)$
50.		920	-	838	924	5.9488	0.8852	756	922	5.2716	0.6725	$\omega\text{CH}(78)+\text{bCC}(22)$
51.		900	-	748	906	0.0710	0.5883	702	903	0.2776	0.4633	$\text{bCC}(79)$
52.		-	890	725	898	0.0323	6.1676	673	895	0.0362	5.6959	$\text{bCC}(79)+\omega\text{CH}(21)$
53.		870	-	619	877	36.3973	0.0634	560	872	26.9794	0.0066	$\omega\text{CH}(80)$
54.		-	820	589	829	0.0664	2.0326	548	821	0.0943	1.5410	$\omega\text{CH}(80)$
55.		810	-	486	814	0.1598	8.1082	454	813	0.1176	5.8639	$\text{CH}_3\text{OPr}(84)$
56.		-	800	471	807	0.0383	0.0320	427	802	0.0429	0.0801	$\text{CH}_3\text{opr}(82)+\omega\text{CH}(18)$
57.		-	730	432	738	1.5290	0.8659	395	735	1.4192	1.0425	$\omega\text{CH}(79)$
58.		710	-	389	715	0.2314	0.4068	363	711	0.2574	0.6247	$\text{CH}_3\text{opr}(79)$
59.		-	690	317	694	0.1179	3.0728	296	692	0.1275	2.9138	$\text{tRSymd}(82)$
60.		-	640	273	643	0.1107	0.0744	259	642	0.1486	0.0962	$\text{tRSymd}(82)$
61.		560	-	252	568	0.2795	1.1264	235	564	0.1386	0.5304	$\omega\text{CC}(79)$
62.		540	-	236	548	0.2199	0.8902	218	544	0.3087	1.3684	$\text{tRtrigd}(74)+\omega\text{CC}(26)$
63.		-	450	206	457	0.3295	0.3744	189	452	0.2500	0.3640	$\omega\text{CC}(82)$
64.		-	390	105	396	1.1038	1.2406	95	393	0.8254	1.5986	$\text{CH}_3\text{twist}(70)+\omega\text{CC}(30)$
65.		-	300	47	308	0.0664	2.9753	38	303	0.0578	3.6299	$\text{CH}_3\text{twist}(70)+\omega\text{CC}(20)$
66.		-	220	32	226	0.1611	0.2360	32	222	0.2467	0.3692	$\text{CH}_3\text{twist}(70)+\omega\text{CC}(20)$

Abbreviations: ν -stretching; ss-symmetric stretching; ips-in-plane stretching; sb-symmetric bending; ipr-in-plane rocking; opr-out-of-plane rocking; ops-out-of-plane stretching; b-bending; ω -out-of-plane bending; R-ring; trigd-trigonal deformation; symd-symmetric deformation; asymd-antisymmetric deformation; t-torsion.

In order to improve the agreement of theoretically calculated frequencies with experimentally calculated frequencies, it is necessary to scale down the theoretically calculated harmonic frequencies. Hence, the vibrational frequencies theoretically calculated at B3LYP/6-311++G(d,p) are scaled down by using MOLVIB 7.0 version written by Tom Sundius [8,9].

4. Results and Discussion

4.1. Optimized Geometry

The optimized molecular structure and the scheme of atoms numbering of IMB is represented in Fig.1. The geometries of IMB under investigation is considered as possessing C_1 point group symmetry. The calculated optimized geometrical parameters of IMB is presented in Table .1 and analyzed as follows.

Several authors have explained the changes in bond length of the C–H bond on substitution due to a change in charge distribution on the carbon of the benzene ring. The substituents may be either of the electron withdrawing type (Cl, F, Br...) or electron donating type (CH_3 , C_2H_5 ,...). The carbon atoms are bonded to the hydrogen atoms with an σ bond in benzene and the substitution of a halogen for hydrogen reduces the electron density at the ring carbon atom. The ring carbon atoms in substituted benzenes exert a larger attraction on the valence electron cloud of the hydrogen atom resulting in an increase in the C–H forces constant and a decrease in the corresponding bond length would be influenced by the combined effects of the inductive-mesomeric interaction and the electric dipole field of the polar substituent.

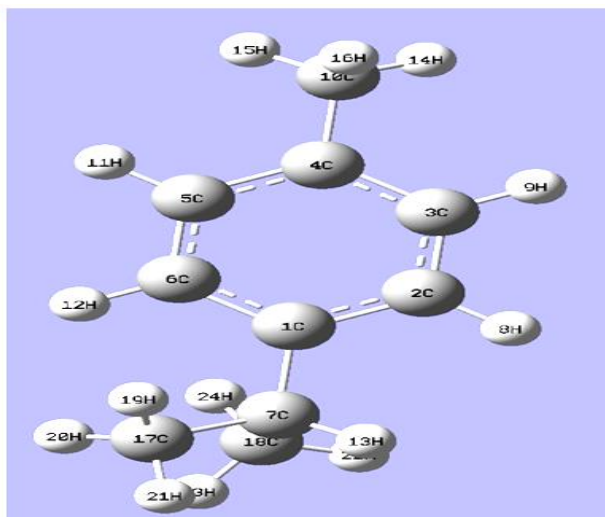


Fig 1. Molecular structure of 1-Isopropyl 4-Methylbenzene.

4.2. Vibrational assignments analysis

The molecule consists of 24 atoms and gives 66 fundamental modes of vibrations. All the vibrational assignments of IMB along with the experimentally and theoretically calculated frequencies are presented in Table 2. The FT-IR and FT-Raman spectra of IMB is shown in Figs. 2-3. The assignments of vibrational frequencies are interpreted as in the following sections.

Since the identification of all normal modes of vibration of compound is not trivial, so to simplify the problem by considering each compound as substituted benzene. Such an idea has already been successfully utilized by several workers for vibrational assignment of compounds containing multiple homo and heteroaromatic rings [10-14].

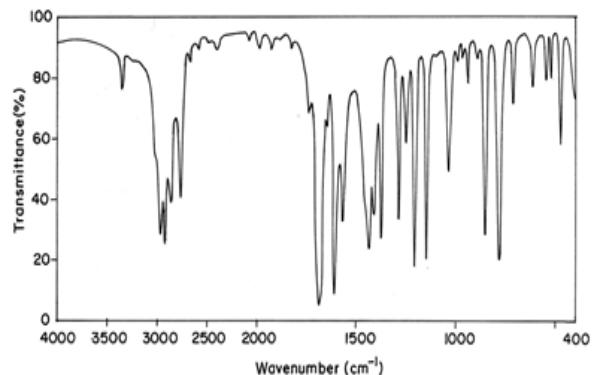


Fig 2. FTIR spectrum of 1-Isopropyl 4-Methylbenzene.

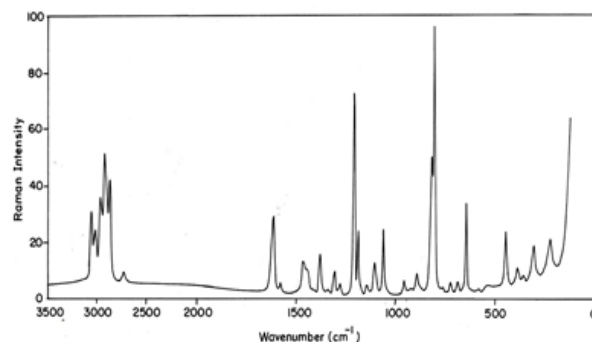


Fig 3. FT-Raman spectrum of 1-Isopropyl 4-Methylbenzene.

C-H vibrations

The heteroaromatic structure shows the presence of C-H stretching vibrations in the region $3100-3000\text{ cm}^{-1}$ [15-17]. This is the characteristic region for the ready identification of C-H stretching vibrations. In this region, the bands are not affected appreciably by the nature of the substitutions. In the present investigation, the C-H stretching vibrations are observed at $3490, 3120, 3050, 3030$, and 2930 cm^{-1} in the FT-IR spectrum and at 3080 and 3020 cm^{-1} in the Raman for IMB. The C-H in-plane and out-of-plane bending vibrations of the IMB have also been identified and listed in Table 2.

C-C vibrations

The benzene possesses six stretching vibrations of which the four with highest wave numbers occurring near $1650-1400\text{ cm}^{-1}$ are good group vibrations [18].

With heavy substituents, the bonds tend to shift to somewhat lower wave numbers and greater the number of substituents on the ring, broader the absorption regions. In the title molecule, the FT-IR bands observed at $1640, 1620, 1510, 1460\text{ cm}^{-1}$ and $1610, 1470\text{ cm}^{-1}$ in FT-Raman have been assigned to C-C stretching vibrations are due to the substituents in benzene ring. The higher percentage of total energy distribution (TED) obtained for this group encouraging and confirms the assignments proposed in this study for C-C stretching vibrations. The in-plane and out-of-plane bending vibrations of C-C group are also listed in Table 2.

Methyl group vibrations

For the assignments of CH_3 group frequencies, basically nine fundamentals can be associated to each CH_3 group namely, CH_3 ss – symmetric stretch; CH_3 ips – in-plane stretch (i.e., in-plane hydrogen stretching modes); CH_3 ipb – in-plane-bending (i.e., hydrogen deformation modes); CH_3 sb – symmetric bending; CH_3 ipr – in-plane rocking; CH_3 opr – out-of-plane rocking and t CH_3 – twisting hydrogen bending modes. In addition to that, CH_3 ops – out-of-plane stretch and CH_3 opb – out-of-plane bending modes of the CH_3 group

would be expected to be depolarised. In the present investigations, the CH₃ ss frequencies are established at 2880 and 2980,2750 cm⁻¹ in IR and Raman Spectrum respectively. The CH₃ips are assigned at 2960 cm⁻¹ and 2970,2940 cm⁻¹ in IR and Raman respectively for IMB. These assignments are also supported by the literature [19,20] in addition to TED output.

The two in-plane methyl hydrogen deformation modes are also well established. We have observed the symmetrical methyl deformation mode CH₃sb, at 1310 and 1300,1280 cm⁻¹ in the infrared and Raman, respectively. The in-plane-bending methyl deformation mode observed at 1570,1410 and 1580 cm⁻¹ in the IR and Raman spectrum respectively. The band at 2740,2600, 1900 cm⁻¹ in infrared is attributed to CH₃ ops and CH₃ opb is observed at 1100 cm⁻¹ and 1110,1060 cm⁻¹ respectively. The methyl deformation modes mainly coupled with the in-plane-bending vibrations.

5. Homo-Lumo Analysis

This electronic absorption corresponds to the transition from the ground to the first excited state and is mainly described by one electron excitation from the highest occupied molecular orbital (HOMO) to the lowest unoccupied molecular orbital (LUMO) [21,22]. The LUMO as an electron acceptor (EA) represents the ability to obtain an electron and HOMO represents ability to donate an electron (ED). The ED groups to the efficient EA groups through π -conjugated path. Many organic molecules containing conjugated π electrons are characterized hyperpolarizabilities are analyzed by means of vibrational spectroscopy [23,24]. In most cases, even in the absence of inversion symmetry, the strongest bands in the Raman Spectrum are weak in the IR spectrum and vice versa. But the intramolecular charge transfer from the donor to acceptor group through a single-double bond conjugate path can include large variations of both molecular dipole moments and molecular polarizability making IR and Raman activity at the same time. The experimental spectroscopic behaviour described above is well accounted for DFT calculations in π -conjugated systems that predict exceptionally large Raman and infrared intensities in IR and Raman spectra are comparable resulting from the electron cloud movement through π -conjugated frame work electron donor to electron acceptor groups. The analysis of wave function indicates that the electron absorption corresponds to the transition from the ground to first excited stated and is mainly described by one electron excitation from the HOMO to LUMO. The atomic orbital compositions of the frontier molecular orbital and few MOS for IMB is sketched in Fig. 4.

E _{HOMO}	= -0.23547 a.u.
E _{LUMO}	= -0.00901 a.u.
Energy gap	= 0.2265 a.u.

The energy gap reflects the chemical activity of the molecules. LUMO as electron acceptor represents the ability to obtain an electron, HOMO represent the ability to donate the electron. Moreover the lower in HOMO–LUMO energy gap explains the eventual charge transfer interactions taking place within the molecules, which influences the biological activity of the molecule.

6. First Hyperpolarizability Calculation

The electronic and vibrational contributions to the first hyperpolarizability have been studied theoretically for many organic and inorganic systems. The values of the first hyperpolarizability were found to be quite large for the so-called push-pull molecules, i.e. p-conjugated molecules with

the electron donating and the electron withdrawing substituents attached to a ring, compared to the mono substituted systems [25]. This type of functionalization of organic materials, with the purpose of maximizing NLO properties, is still commonly followed route.

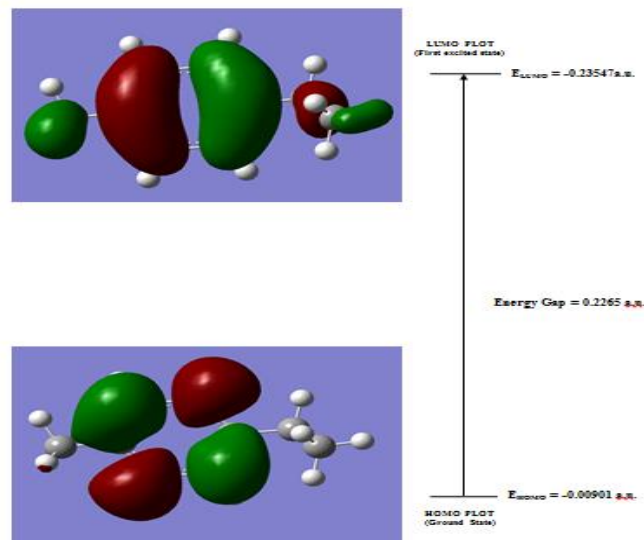


Fig 4. The atomic orbital of HOMO-LUMO composition of frontier molecular orbital for 1-Isopropyl-4-Methylbenzene.

The first hyperpolarizability of title compound is calculated using DFT and HF methods with 6-311++G(d,p) basis set. In the presence of an applied electric field, the energy of a system is a function of the electric field. First order hyperpolarizability (β) is a third rank tensor that can be described by $3 \times 3 \times 3$ matrices. The components of β are defined as the coefficients in the Taylor series expansion of the energy in the external electric field. When the external electric field is weak and homogeneous, this expansion becomes:

$$E = E^0 - \mu_\alpha F_\alpha - \frac{1}{2} \alpha_{\alpha\beta} F_\alpha F_\beta - \frac{1}{6} \beta_{\alpha\beta\gamma} F_\alpha F_\beta F_\gamma + \dots \quad (1)$$

where E^0 is the energy of the unperturbed molecule, F_α is the field at the origin, and μ_α , $\alpha_{\alpha\beta}$ and $\beta_{\alpha\beta\gamma}$ are the components of dipole moment, polarizability and the first order hyperpolarizability, respectively. The total static dipole moment (μ) and the mean first hyperpolarizability (β) using the x, y, z components, they are defined as:

$$\mu = (\mu_x^2 + \mu_y^2 + \mu_z^2)^{1/2}$$

$$\beta = (\beta_x^2 + \beta_y^2 + \beta_z^2)^{1/2}$$

where

$$\beta_x = \beta_{xxx} + \beta_{xyy} + \beta_{zzz}$$

$$\beta_y = \beta_{yyy} + \beta_{xxy} + \beta_{yzz}$$

$$\beta_z = \beta_{zzz} + \beta_{xxz} + \beta_{yyz}$$

Since the value of hyperpolarizability (β) of the GAUSSIAN 09W output is reported in atomic units (a.u.), the calculated values should have been converted into electrostatic units (esu) (β : 1 a.u. = 8.639×10^{-33} e.s.u.). The total molecular dipole moment and first hyperpolarizability are 0.0641 Debye and 0.7336×10^{-30} e.s.u., respectively and are depicted in Table 3.

Table 3.The calculated first hyperpolarizability (β) of 1-isopropyl -4- methyl benzene using DFT/ B3LYP/6-311++G(d,p) method and basis set.

Parameters	1-Isopropyl -4- methyl benzene
β_{xxx}	5.7434157
β_{xxy}	-26.4915551
β_{xyy}	-45.4421044
β_{yyy}	-44.0642854
β_{xxz}	12.6781007
β_{yyz}	-9.106822
β_{xzz}	-16.6890597
β_{yzz}	-17.0475786
β_{zzz}	-7.0345488
β	0.7336×10^{-30}
Dipole moment	0.0641 Debye

7. Thermodynamical Parameters

Several calculated thermodynamical parameters, rotational constants, rotational temperature and vibrational temperature have been presented in Table 4. The zero-point vibration energies, the entropy and the molar capacity at constant volume were calculated. The variations in the zero-point vibration energies seem to be insignificant. The changes in the total entropy of IMB at room temperature at DFT/6-311++G(d,p) and HF/6-311++G(d,p) methods are only marginal [26].

Table 4. The thermodynamical parameters 1-Isopropyl -4- methyl benzene calculated at the HF/6-311++G(d,p) and B3LYP/6-311++G(d,p) methods and basis set.

Parameters	1-Isopropyl-4-methylbenzene	
	HF 6-311++G(d,p)	B3LYP 6-311++G(d,p)
Zero point vibrational energy (Kcal/Mol)	143.28838	134.31455
Rotational constants (GHZ)		
A	3.28881	3.23443
B	0.72619	0.71789
C	0.68570	0.67703
Entropy (Cal/Mol-Kelvin)	98.941	101.591
Specific heat capacity at constant volume (Cal/Mol-Kelvin)	35.974	38.888
Total (Thermal) energy (KCal/Mol)	149.456	140.873
Translational energy (KCal/Mol)	0.889	0.889
Rotational energy (KCal/Mol)	0.889	0.889
Vibrational energy (KCal/Mol)	147.679	139.096
Dipole moment (Debye)	0.0370	0.0641

8. Conclusion

The FT-IR and FT-Raman spectra of 1-isopropyl-4-methylbenzene have been studied. The equilibrium geometries, harmonic wavenumbers and HF and DFT calculations for IMB is carried out for the first time. Optimized geometrical parameters of the title compound are calculated. B3LYP/6-311++G(d,p) calculations are shown better correlation with the experimental data than other calculations. The calculated vibrational values are in good agreement when they are compared with IR and Raman experimental data. Frontier molecular orbital analysis, and NLO properties and other molecular properties of the title compound are also studied at DFT/6-311++G(d,p) and HF/6-311++G(d,p) levels. The results of this study will help researches to design and synthesis of new materials. Decrease in HOMO and LUMO energy gap, explains the eventual charge transfer within the molecule which is responsible for the chemical reactivity of the molecule. These calculations are carried out in ground state by using *ab initio* and Density functional theory.

References

- [1] Q. Zhu, X.M. Zhang, A.J. Fry, *Polymer Degradation and Stability* 57 (1997) 43.
- [2] L. Quaroni, W.E. Smith, *J. Raman Spec.* 30 (1999) 537.
- [3] L. Quaroni, J. Reglinski, R. Wolf, W.E. Smith, *Biochim Biophysica Acta* 1296 (1996) 5.
- [4] L. Quaroni, W.E. Smith, *Biospec.* 5 (1999) S71.
- [5] V.G. Osipov, V.A. Shlyapochnikov, E.F. Ponzovtsev, *J. App. Spec.* 8 (1968) 1003.
- [6] J.H.S. Green, W. Kynaston, A.S. Lindsay, *Spectrochim Acta* 17 (1961) 933.
- [7] M.J. Frisch, G.W. Trucks, H.B. Schlegel et al., GAUSSIAN 09W, Revision A.02, Gaussian, Inc., Wallingford CT, 2009.
- [8] T. Sundius, Molvib (V.70): "Calculation of Harmonic Force Fields and Vibrational Modes of Molecules", QCPE Program No., 807, 2002.
- [9] T. Sundius, *Vib. Spectrosc.* 29 (2002) 89.
- [10] P. Sett, N. Paul, S. Chattopadhyay, PK. Mallick, *J. Raman spectrosc.* 30(1999) 277.
- [11] P. Sett, N. Paul, S. Chattopadhyay, PK. Mallick, *Spectrochim. Acta A* 56 (2000) 855.
- [12] P. Sett, N. Paul, S. Chattopadhyay, PK. Mallick, *J. Raman spectrosc.* 31 (2000) 177.
- [13] V. Volvosek, G. Baranovic, L. Colombo, JR. Durig, *J. Raman Spectrosc.* 22 (1991) 35.
- [14] M. Muniz-Miranda, E. Castelluci, N. Neto, G. Sbrena, *Spectrochim Acta A* 39 (1983) 107.
- [15] Silverstein R M, Clayton Basseler G, Morrill, *Spectrometric identification of Organic Compounds*, John Wiley and Sons, New York, 1991.
- [16] Balamurugan N, Charanya C, Sampath Krishnan S, Muthu S, *Spectrochim. Acta A* 137 (2015) 1374.
- [17] Vijayakumar T, Joe H, Nair C P R, Jayakumar V S, *J. Chem. Phys.* 343 (2008) 83.
- [18] Socrates G, *IR and Raman Characteristics Group Frequencies Tables and Charts*, 3rd ed., Wiley, Chichester (2001) 107.
- [19] Krishnakumar V and Balachandran V, *Spectrochim Acta Part A*, 61 (2005) 2510.
- [20] John Xavier R, Balachandran V, Arivazhagan M and Ilango G, *Indian J. Pure and Appl. Phys.*, 48 (2010) 245.
- [21] Kavitha E, Sundaraganesan N & Sebastin S, *Indian J. Pure & App. Physics*, (2010) 20.
- [22] Y. X. Sun, Q.-L. Hao, Z.-X. Yu, W.-J. Jiang, L.-D. Lu, X. Wang, *Spectrochim Acta A* 73 (2009) 892.
- [23] T. Vijayakumar, Hubert. Joe, C.P.R. Nair, V.S. Jayakumar, *Chem. Phys.*, 343 (2008) 83.
- [24] Y. Atalay, D. Avil, A. Basaoglu, *Struct. Chem.*, 19 (2008) 239.
- [25] R. Zalesny et al., *THEOCHEM* 907 (2009) 46.
- [26] M. Alcolea, Palafox *Int. J. Quant. Chem.*, 77 (2000) 661.